Elastic lattice deformation in quantum-wire heterostructures

Liberato De Caro and Leander Tapfer
Centro Nazionale Ricerca e Sviluppo Materiali (CNRSM), Strada Statale 7 Appia km 712, I-72100 Brindisi, Italy
(Received 20 December 1993)

We report on the lattice deformation of quantum-wire heterostructures with cubic symmetry deposited on arbitrarily oriented substrate surfaces. The elasic strain and the stress-tensor components are calculated by using Hooke's law and applying the appropriate boundary conditions at the wire-substrate interface. We assume that the lattice coherence at the wire-substrate interface is achieved only along the wire direction, due to the limted lateral extension of the wires. We show that either a tetragonal or an orthorhombic or a lower-symmetry lattice deformation of the quantum-wire structure may occur depending on the coherence direction and substrate orientation. In some particular cases, even for high-symmetry substrate orientations ([001] and [110]), it is possible to obtain one shear strain element different from zero, leading to a monoclinic lattice deformation. Moreover, for the [111] or low-symmetry substrate orientations a triclinic lattice deformation can also be obtained. In the case of an orthorhombic lattice deformation our theoretical results are found to be in good agreement with the few experimental data available.

I. INTRODUCTION

The lattice deformation and the strain fields, generated by the lattice mismatch between different material systems of semiconductor heterostructures, affect both the microscopic[1,2] and the macroscopic properties of the crystals.[3] Therefore, it is of great importance for the design and development of new optoelectronic and electronic devices to determine quantitatively the stress and the strain fields of the crystalline heterostructures. In the case of layered structures grown pseudomorphically on thick substrate crystals, the elastic lattice deformation is characterized by the evidence that the in-plane lattice mismatch between film and substrate is zero, i.e., the lattice constant of the heterostructures is accommodated to the lattice parameter of the substrate in all in-plane directions. It is well known that coherent heterostructures can be realized as long as the thickness of the whole epitaxial structure does not exceed the critical thickness.[4] Relaxation phenomena which modify strain fields were also observed in semiconductor structures with reduced spatial dimensions.[5,6] In particular, structure relaxation is very important for low-dimensional systems, such as quantum wires, which are of great current interest due to their unique physical properties and potential optoelectronic device applications.

The stress and strain status of heterostructures can be determined by solving the equations of the elasticity theory using Hooke's law and appropriate boundary conditions. Very recently, we calculated the strain tensor elements of strained arbitrarily-oriented cubic epitaxial layers by minimizing the strain energy density via the commensurability constraint.[7]

In this paper (Sec. II), we obtain the general expressions for the strain and the stress fields of a quantum-wire heterostructure with cubic symmetry on an arbitrarily-oriented substrate crystal with a different lattice constant, assuming that the coherence between the wire and the substrate lattices holds only along the wire direction. In Sec. III, the lattice deformations have been analyzed as a function of the substrate orientation and the wire direction. Important differences with respect to the tetragonal lattice deformation[7] are elucidated and discussed. Finally, in Sec. IV, it is shown that, in the case of an orthorhombic lattice deformation the theoretical results, are in good agreement with the few available experimental results[5,6] on the lattice deformations in quantum-wire heterostructures.

II. BOUNDARY CONDITIONS FOR UNIDIMENSIONAL HETEROSTRUCTURES AND SOLUTION OF THE ELASTICITY EQUATIONS

Let us consider a quantum wire of crystalline material on an arbitrarily-oriented lattice-mismatched substrate crystal, such as the one shown in Fig. 1. If we consider a crystalline elastic medium with cubic symmetry, which obeys Hooke's law and is defect free, the elasticity equations can be written as

$$\varepsilon_i = S_{ij}\sigma_j \ , \tag{1}$$

with $i,j=\{1,\ldots,6\}$ in the contracted matrix notation.[8] Here ε_i, S_{ij}, and σ_j are the strain, the compliance and the stress matrix components, respectively, with respect to the "interface" coordinate system $\mathbf{x}_1$, $\mathbf{x}_2$, and $\mathbf{x}_3$ as shown in Fig. 1. The axis $\mathbf{x}_2$ is directed along the wire, while the axis $\mathbf{x}_3$ is normal to the interface between the quantum wire and substrate. We have chosen the interfacial reference system $\{\mathbf{x}_i\}$ rather than the crystallographic reference system $\{\mathbf{y}_k\}$, shown in Fig. 1, because in this way it is easier to define the boundary conditions.

In order to describe the lattice distortion of the wire structure correctly, several assumptions have to be made.

(i) If the wire width is much smaller than the wire length, we assume that the lattice coherence between the

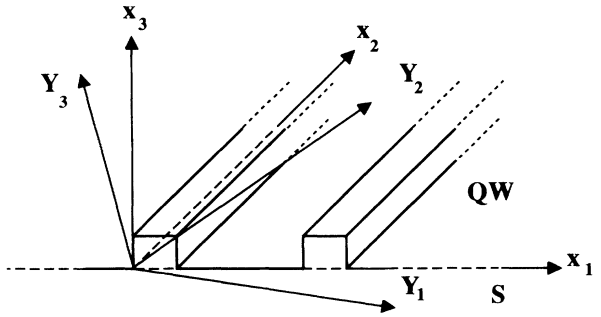

FIG. 1. Schematic diagram of a quantum-wire structure deposited onto a substrate crystal of arbitrary surface orientation. $\{\mathbf{y}_i\}$ denotes the crystallographic reference system, while $\{\mathbf{x}_i\}$ denotes the "interface" one, individuated by the wire direction and the normal to the interface.

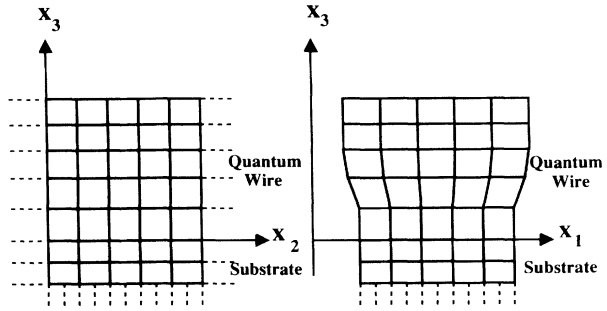

FIG. 2. Schematic diagram of the elastic match between the orthorhombic and the tetragonal lattice deformations, near the interface.

wire and substrate holds only along the wire direction ($\mathbf{x}_2$-axis), whereas, along the other two orthogonal directions, the wire lattice may deform elastically until the stresses that act along these directions go to zero. It should be noted that, in real cases, this condition should be valid for almost all the quantum-wire lattice, but not for a narrow region, near the interface, where the coherence condition should be valid for *all* in-plane directions, as in the pseudomorphic growth (see Fig. 2). In other words, neglecting some monolayers near the interface, the strain field should be uniform and is determined by the unidimensional coherence condition. In Sec. IV we will show that this assumption can be verified in real structures.

(ii) The quantum-wire height is much smaller than the critical thickness in order to deal with elastic deformations only.

(iii) The quantum-wire height is much smaller than the substrate thickness and, therefore, all the strain occurs in the wire.

Thus, we can define the following boundary conditions:

$$\begin{aligned} &\sigma_1=\sigma_3=\sigma_4=\sigma_5=\sigma_6=0\ , \\ &\varepsilon_2=\varepsilon^{\parallel}\ . \end{aligned} \tag{2}$$

Here $\varepsilon^{\parallel}=(a_s-a_w)/a_w$, where a_s and a_w are the lattice constants of the substrate and the wire, respectively. Using the constraints in Eq. (2), we obtain the following solution for the elasticity equations:

$$\begin{aligned} &\varepsilon_i=\frac{S_{i2}}{S_{22}}\varepsilon^{\parallel}\ , \\ &\sigma_2=\frac{1}{S_{22}}\varepsilon^{\parallel}\ , \end{aligned} \tag{3}$$

with $i=\{1,\ldots,6\}$.

In order to obtain the compliance tensor components in the reference system $\{\mathbf{x}_i\}$, we use the equations given by Anastassakis and Liarokapis,[9] which relate them to the corresponding components in the crystallographic reference system $\{\mathbf{y}_k\}$. We can express the compliance tensor components in terms of stiffness components and Eq. (3) can be written as

$$\begin{aligned} \varepsilon_j&=\frac{2C_{12}C_{44}+C(C_{11}+2C_{12})R_{j2}}{2C_{12}C_{44}+C(C_{11}+2C_{12})R_{22}-(C_{11}+2C_{12})(C_{11}-C_{12})}\varepsilon^{\parallel}\ , \\ (\varepsilon_s)_i&=\frac{C(C_{11}+2C_{12})R_{i2}}{2C_{12}C_{44}+C(C_{11}+2C_{12})R_{22}-(C_{11}+2C_{12})(C_{11}-C_{12})}\varepsilon^{\parallel}\ , \\ \sigma_2&=\frac{-2C_{44}(C_{11}+2C_{12})(C_{11}-C_{12})}{2C_{12}C_{44}+C(C_{11}+2C_{12})R_{22}-(C_{11}+2C_{12})(C_{11}-C_{12})}\varepsilon^{\parallel}\ . \end{aligned} \tag{4}$$

Here, the ε_j with $j=\{1,3\}$ are the no-trivial diagonal strain tensor components, $(\varepsilon_s)_i$ are the shear strain tensor elements with $i=\{4,5,6\}$, C_{jk} are the stiffness constants, $C=C_{11}-C_{12}-2C_{44}$, and σ_2 is the only no-null stress component along the wire direction. The coefficients R_{jk} are given by

$$R_{jk}=T_{\alpha 1}T_{\beta 1}T_{\gamma 1}T_{\delta 1}+T_{\alpha 2}T_{\beta 2}T_{\gamma 2}T_{\delta 2}+T_{\alpha 3}T_{\beta 3}T_{\gamma 3}T_{\delta 3}\ , \tag{5}$$

where $T_{\alpha\beta}$ is the transformation matrix from $\{\mathbf{y}_k\}$ to $\{\mathbf{x}_i\}$ and $j,k=\{1,\ldots,6\}$ indicate in a contracted notation the pairs of indices $\alpha\beta$ and $\gamma\delta=\{1,2,3\}$, respectively.[8,9]

Equations (2) and (4) give the stress and the strain fields for a quantum-wire lattice with cubic symmetry on an arbitrarily-oriented lattice-mismatched substrate.

Denoting with $(\Delta d/d)_{\parallel}$ the lattice mismatch in the interface plane $(\mathbf{x}_1,\mathbf{x}_2)$, normal to the wire direction $\mathbf{x}_2$, and with $(\Delta d/d)_{\perp}$ the lattice mismatch normal to the interface plane (along the $\mathbf{x}_3$ axis), we obtain the following relations:

$$(\Delta d/d)_{\parallel}=\varepsilon^{\parallel}-\varepsilon_1=\frac{(C_{11}+2C_{12})[C_{12}-C_{11}+C(R_{22}-R_{12})]}{2C_{12}C_{44}+C(C_{11}+2C_{12})R_{22}-(C_{11}+2C_{12})(C_{11}-C_{12})}\varepsilon^{\parallel}\ ,$$
$$(\Delta d/d)_{\perp}=\varepsilon^{\parallel}-\varepsilon_3=\frac{(C_{11}+2C_{12})[C_{12}-C_{11}+C(R_{22}-R_{32})]}{2C_{12}C_{44}+C(C_{11}+2C_{12})R_{22}-(C_{11}+2C_{12})(C_{11}-C_{12})}\varepsilon^{\parallel}\ . \tag{6}$$

Obviously, along the wire direction ($\mathbf{x}_2$-axis) we have an in-plane lattice mismatch equal to zero, as defined by the constraints [Eq. (2)]. Therefore, due to the partial elastic relaxation, only if $(\Delta d/d)_{\parallel}=(\Delta d/d)_{\perp}$ and all the off-diagonal strain components are equal to zero, we obtain a tetragonal lattice deformation, as we will see in the next section.

III. LATTICE DEFORMATION

The deformation of the unit cell of the quantum wires caused by the lattice mismatch depends on the substrate surface orientation as well as on the wire direction. It is interesting to note that in the case of strained epitaxial layers, we have obtained a tetragonal lattice deformation for all high-symmetry substrate orientations ([001], [110], and [111]), being all the off-diagonal components of the strain tensor $(\varepsilon_i)_s$ equal to zero.[7] Moreover, in the case of strained epitaxial layers, for low-symmetry substrate orientations the lowest-symmetry lattice deformation is monoclinic. In fact, in this case $\varepsilon_6=0$ is a boundary condition, and one of the principal axes of the strain matrix always belongs to the interface plane $(\mathbf{x}_1,\mathbf{x}_2)$.[7] This leads to the possibility of choosing an opportune pair $(\mathbf{x}_1,\mathbf{x}_2)$ of axes for which only one off-diagonal strain component is different from zero for any substrate orientation.

On the contrary, we will show, that for lateral confined heterostructures the situation is much more complicated in the case of high-symmetry substrate orientations.

A. [001]-ORIENTED SUBSTRATES

If the substrate surface is normal to the [001] direction, we can choose the three coordinate axes $\{\mathbf{x}_i\}$ as follows: $\mathbf{x}_1\|[jk0]$, $\mathbf{x}_2\|[\bar{k}j0]$, and $\mathbf{x}_3=[001]$, where j and k are integers. Thus, from the Eq. (5) it follows that

$$R_{42}=0, R_{52}=0, R_{62}\propto kj^3-jk^3\ , \tag{7a}$$

$$R_{32}=0, R_{12}\propto j^2k^2\ . \tag{7b}$$

Therefore, a sufficient condition for having null off-diagonal strain tensor components $(\varepsilon_i)_s$ is $R_{62}=0$. This can be achieved by putting in the Eqs. (7a) and (7b) either $j=k=1$ or $j=0$ or $k=0$. In this way, the lattice deformation is either orthorhombic ($R_{12}\neq R_{32}=0$, for $j=k=1$) or tetragonal ($R_{12}=R_{32}=0$, for $j=0$ or $k=0$), depending on the particular wire direction. For example, if $\mathbf{x}_2=[\bar{1}00]$ from Eq. (6) we have a tetragonal lattice deformation:

$$(\Delta d/d)_{\parallel}=(\Delta d/d)_{\perp}=\frac{(C_{11}+2C_{12})}{(C_{11}+C_{12})}\varepsilon^{\parallel}\ . \tag{8}$$

This is due to the fact, that both the lateral and normal lattice relaxations occur along equivalent crystallographic directions. However, if $\mathbf{x}_2\|[\bar{1}10]$ we have an orthorhombic deformation:

TABLE I. Lattice deformation as a function of the wire direction for high-symmetry ([001], [110], and [111]) substrate orientations.

Substrate orientation ($\mathbf{x}_3$)	Wire direction ($\mathbf{x}_2$)	Lateral direction of partial elastic relaxation ($\mathbf{x}_1$)	Lattice deformation
[001]	$[\bar{1}00]$	[010]	tetragonal
[001]	$[\bar{1}10]$	[110]	orthorhombic
[001]	$[\bar{k}j0]$	$[jk0]$	monoclinic
[110]	[001]	$[\bar{1}10]$	tetragonal
[110]	$[1\bar{1}0]$	[001]	orthorhombic
[110]	$[1\bar{1}1]$	$[\bar{1}12]$	tetragonal
[110]	$[j\bar{j}k]$	$[\bar{k}k2j]$	monoclinic
[111]	$[10\bar{1}]$	$[1\bar{2}1]$	monoclinic
[111]	$[01\bar{1}]$	$[2\bar{1}\bar{1}]$	monoclinic
[111]	$[11\bar{2}]$	$[1\bar{1}0]$	monoclinic
[111]	$[j,k,-(h+k)]$	$[2k+j,-(2j+k),j-k]$	triclinic

$$(\Delta d/d)_{\parallel}=\varepsilon^{\parallel}-\varepsilon_1=\frac{2(C_{11}+2C_{12})(C_{11}-C_{12})}{(C_{11}+2C_{12})(C_{11}-C_{12}+2C_{44})-4C_{12}C_{44}}\varepsilon^{\parallel}\ ,$$
$$(\Delta d/d)_{\perp}=\varepsilon^{\parallel}-\varepsilon_3=\frac{(C_{11}+2C_{12})(C_{11}-C_{12}+2C_{44})}{(C_{11}+2C_{12})(C_{11}-C_{12}+2C_{44})-4C_{12}C_{44}}\varepsilon^{\parallel}\ . \tag{9}$$

On the other hand, if $j\neq k$ (with $k\neq 0$ and $j\neq 0$) the strain tensor, as a function of the coherence direction, can have $\varepsilon_6\neq 0$, leading to a monoclinic lattice deformation, contrary to the case of strained epitaxial layers.[7] These results are summarized in Table I.

In Fig. 3(a) we can see the normalized lattice deformations $(\Delta d/d)_{\perp}/\varepsilon^{\parallel}$ and $(\Delta d/d)_{\parallel}/\varepsilon^{\parallel}$, for two families of quantum-wire orientations: $[\bar{k},1,0]$ with k integer if $0\leq T_{22}\leq 1/\sqrt{2}$ and $[\bar{1},k,0]$ with k integer if $1/\sqrt{2}\leq T_{22}\leq 1$. Here, simply we used the GaAs stiffness constants.[10] It should be noted that in this way the normalized strains are independent of the lattice mismatch $\varepsilon^{\parallel}$. Therefore, the normalized strains for different material systems depend only on the stiffness constants. From the results reported in Fig. 3(a), we can see that $(\Delta d/d)_{\perp}/\varepsilon^{\parallel}\neq(\Delta d/d)_{\parallel}/\varepsilon^{\parallel}$ for each low-symmetry quantum-wire direction, as reported in Table I. The maximum value for $(\Delta d/d)_{\perp}/\varepsilon^{\parallel}$ (about 1.43) coincides with the minimum value for $(\Delta d/d)_{\parallel}/\varepsilon^{\parallel}$ (about 1.02), when $\mathbf{x}_2\|[\bar{1}10]$.

In Fig. 3(b) the normalized shear strain components $(\varepsilon_i)_s/\varepsilon^{\parallel}$ are reported as a function of T_{22} for the same families of quantum-wire orientations. From this figure we can see that only one shear strain component can be different from zero for low-symmetry quantum-wire directions, as indicated in Table I, too. The shear strain component can also reach about the 16% of the value of $\varepsilon^{\parallel}$ for the quantum-wire orientations $[\bar{1}20]$ and $[\bar{2}10]$.

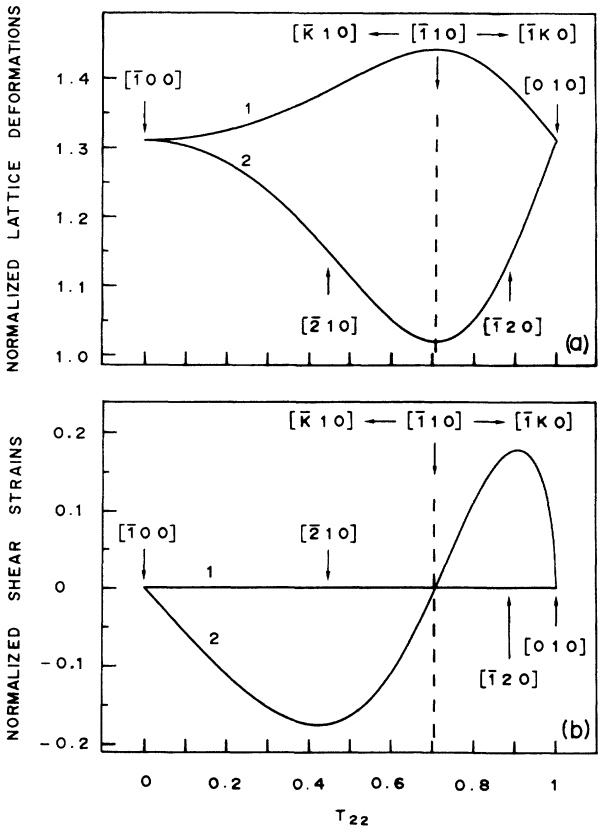

FIG. 3. (a) Normalized lattice deformations $(\Delta d/d)_{\perp}/\varepsilon^{\parallel}$ (curve 1) $(\Delta d/d)_{\parallel}/\varepsilon^{\parallel}$ (curve 2), for a GaAs layer grown on a [0,0,1]-oriented lattice-mismatched substrate, for two families of quantum-wire orientations: $[\bar{k},1,0]$ with a k integer if $0\leq T_{22}\leq 1/\sqrt{2}$; $[\bar{1},k,0]$ with a k integer if $1/\sqrt{2}\leq T_{22}\leq 1$; (b) normalized shear strain components $(\varepsilon_4)_s/\varepsilon^{\parallel}=(\varepsilon_5)_s/\varepsilon^{\parallel}$ (curve 1) and $(\varepsilon_6)_s/\varepsilon^{\parallel}$ (curve 2), for a GaAs layer grown on a [0,0,1]-oriented lattice-mismatched substrate, for the same families of quantum-wire orientations.

B. [110]-oriented substrates

If the substrate orientation is $\mathbf{x}_3\|[110]$, we can put $\mathbf{x}_1\|[\bar{k},k,2j]$, $\mathbf{x}_2\|[j,\bar{j},k]$, where j and k are integers. In this case, the condition for having all $(\varepsilon_i)_s=0$ does not change [Eq. (7a)]. However, Eq. (7b) becomes

$$R_{32}=j^2/(k^2+2j^2)\ ,\quad R_{12}=3j^2k^2/(k^2+2j^2)^2\ . \tag{10}$$

Therefore, if $j=0$ or $j=k=1$, we have $R_{32}=R_{12}$, $R_{26}=0$ and, consequently, the deformation field is tetragonal. Otherwise, if $k=0$ and $j\neq 0$, the deformation field is orthorhombic. Moreover, as for the [001]-substrate case, if $j\neq k$ and $k\neq 0$ and $j\neq 0$, the lattice deformation becomes monoclinic (see Table I).

These results can be seen very clearly in Figs. 4(a) and 4(b). Figure 4(a) shows the normalized lattice deformations $(\Delta d/d)_{\perp}/\varepsilon^{\parallel}$ and $(\Delta d/d)_{\parallel}/\varepsilon^{\parallel}$, for two families of quantum-wire orientations: $[k,\bar{k},1]$ with k integer if $0\leq T_{23}\leq 1/\sqrt{3}$ and $[1,\bar{1},k]$ with k integer if $1/\sqrt{3}\leq T_{23}\leq 1$. Here, the GaAs stiffness constants are used for the calculation. From this figure we can see that $(\Delta d/d)_{\perp}/\varepsilon^{\parallel}\neq(\Delta d/d)_{\parallel}/\varepsilon^{\parallel}$ for each low-symmetry quantum-wire direction and for the high-symmetry $[1\bar{1}0]$ direction, as reported in Table I. For the high-symmetry $[1\bar{1}0]$ direction, we find the minimum value for $(\Delta d/d)_{\parallel}/\varepsilon^{\parallel}$ (about 1.02) and the maximum value for $(\Delta d/d)_{\perp}/\varepsilon^{\parallel}$ (about 1.45).

In Fig. 4(b) the normalized shear strain components $(\varepsilon_i)_s/\varepsilon^{\parallel}$ are shown as a function of T_{23} for the same families of quantum-wire orientations. For low-symmetry quantum-wire directions, only one shear strain component can be different from zero, as indicated in Table I, too. The maximum absolute value of $(\varepsilon_6)_s$ is about 22% of $\varepsilon^{\parallel}$.

C. [111]-oriented substrates

If the substrate orientation is $\mathbf{x}_3\|[111]$, it is not possible to have a tetragonal lattice deformation for any in-

plane quantum-wire direction, due to the fact that there is no crystallographic direction equivalent to the $\mathbf{x}_3$ axis which is normal to it. Thus, in contrast to the cast of pseudomorphic growth of strained epitaxial layers,[7] the highest-symmetry lattice deformation for a [111]-oriented substrate is not tetragonal but monoclinic. In fact, using the conditions $R_{1k}+R_{2k}+R_{3k}=1$ for $k\in\{1,2,3\}$ (Ref. 9) and the orthogonality condition of $\mathbf{x}_2$ with respect to the axis $\mathbf{x}_3$ ($j+k+m=0$), it can be easily verified that, for any possible quantum-wires direction $\mathbf{x}_2\|[jkm]$ in the interface plane, one always has $R_{62}=0$, $R_{23}=\frac{1}{3}$, $R_{12}=\frac{1}{2}$, and $R_{22}=\frac{1}{6}$. This implies that $(\Delta d/d)_\perp/\varepsilon^\parallel=1.161$ and $(\Delta d/d)_\parallel/\varepsilon^\parallel=1.302$ for any $\mathbf{x}_2$. Therefore, we can never obtain a tetragonal deformation. Moreover, in order to have at least an orthorhombic deformation we should also have $R_{42}=R_{52}=0$. These two conditions, however, cannot be achieved simultaneously for any $\mathbf{x}_2\|[j,k,-j-k]$.

These results can be seen clearly in Fig. 5, where the normalized shear strains $(\varepsilon_i)_s$ for the quantum-wire orientations $[k,1,-1-k]$ with k integer and with $0<T_{22}\le 1/\sqrt{2}$ is reported. From Fig. (5) it follows that if $\mathbf{x}_2\|[10\bar{1}]$ or $\mathbf{x}_2\|[01\bar{1}]$ or $\mathbf{x}_2\|[11\bar{2}]$ only one shear strain is different from zero and, therefore, the deformation is monoclinic. In this case, it is possible to reach the maximum absolute value for the shear strains, which is about 20% of $\varepsilon^\parallel$. For any other orientation belonging to the family $[j,k,-j-k]$, we obtain that two shear strains are different from zero, leading to a triclinic deformation.

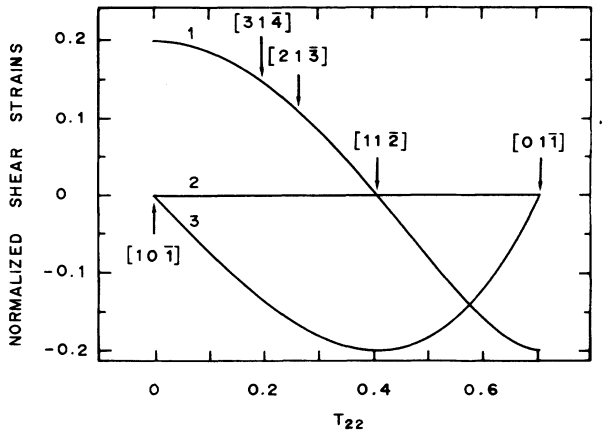

FIG. 5. Normalized shear strain components $(\varepsilon_5)_s/\varepsilon^\parallel$ (curve 1), $(\varepsilon_6)_s/\varepsilon^\parallel$ (curve 2), and $(\varepsilon_4)_s/\varepsilon^\parallel$ (curve 3), for a GaAs layer grown on a [1,1,1]-oriented lattice-mismatched substrate, for the family of quantum-wire orientations $[k,1,-(1+k)]$ with k integer and $0\le T_{22}\le 1/\sqrt{2}$.

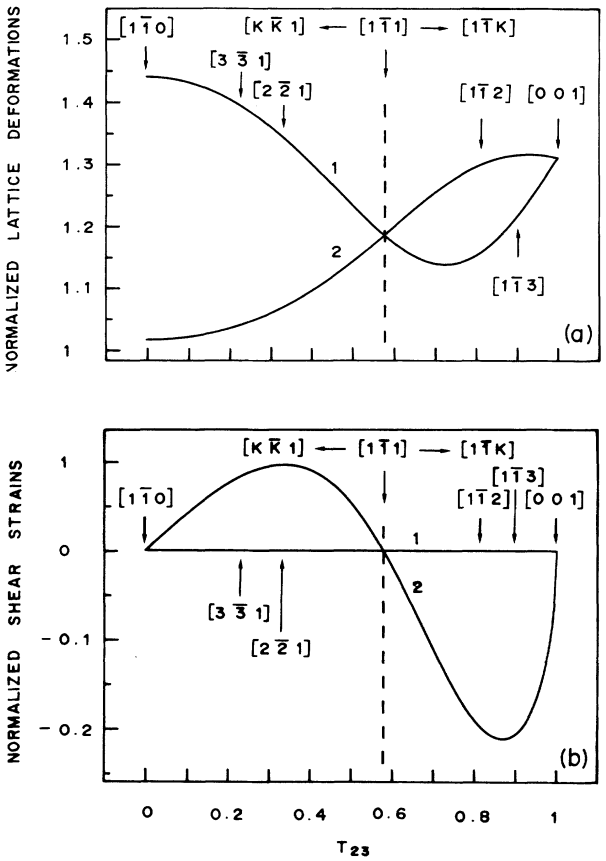

FIG. 4. (a) Normalized lattice deformations $(\Delta d/d)_\parallel/\varepsilon^\parallel$ (curve 1) and $(\Delta d/d)_\perp/\varepsilon^\parallel$ (curve 2), for a GaAs layer grown on a [1,1,0]-oriented lattice-mismatched substrate, for two families of quantum-wire orientations: $[k,\bar{k},1]$ with a k integer if $0\le T_{23}\le 1/\sqrt{3}$; $[1,\bar{1},k]$ with a k integer if $1/\sqrt{3}\le T_{23}\le 1$; (b) normalized shear strain components $(\varepsilon_4)_s/\varepsilon^\parallel=(\varepsilon_5)_s/\varepsilon^\parallel$ (curve 1) and $(\varepsilon_6)_s/\varepsilon^\parallel$ (curve 2), for a GaAs layer grown on a [1,1,0]-oriented lattice-mismatched substrate, for the same families of quantum-wire orientations.

D. Low-symmetry oriented substrates

From Eqs. (4) and (5) we obtain that for lower-symmetry substrate orientations the highest-symmetry lattice deformation is also monoclinic. On the other hand, all the shear strain elements can be different from zero, giving rise to a triclinic lattice deformation. These results are clearly different from those obtained in the case of the pseudomorphic grown epitaxial layers, where the lowest-symmetry lattice deformation is monoclinic.[7]

IV. THEORETICAL RESULTS VERSUS EXPERIMENTAL EVIDENCES

Now, we will compare the results of our model with the few available experimental data. Tapfer *et al.*[5] reported on the asymmetrical (224) diffraction pattern measurements of an InAs/GaAs quantum-wire structure, directed along the [110] direction, fabricated on a (001) GaAs substrate. This quantum-wire structure was obtained by reactive ion etching of a pseudomorphic MBE (molecular-beam epitaxy) grown InAs/GaAs superlattice composed of 10 periods. All the structural parameters of the quantum wire obtained from the analysis of the x-ray-diffraction data, are given in Ref. 5. In another paper, Tapfer *et al.*[6] reported on double crystal x-ray-diffraction measurements of an $Al_{0.36}Ga_{0.64}As/GaAs$ quantum-wire structure, directed along the [110] direction, on a (001) $Al_{0.36}Ga_{0.64}As$ buffer layer. These quantum wires were obtained by an ion etching process of a

pseudomorphic MBE grown $Al_{0.36}Ga_{0.64}As/GaAs$ multiple quantum well (25 periods).

It is important to note that before etching the average in-plane lattice distortion in one period is zero for both the cases, indicating a coherent epitaxial structure-substrate interface. The results for the average lattice strain along the [001] axis are summarized in the third column of Table II.

The diffraction measurements, performed after the etching process, reveal that the average lattice strain along the [001] axis is reduced, and the presence of an in-plane lattice strain different from zero perpendicular to the wire direction is evidenced. In other words, the diffraction data reveal a partial strain relaxation of the quantum-wire structure. The experimental values are reported in Table II, where EL refers to the film before the etching process, while QW refers to the quantum-wire structure.

In order to reproduce the above-mentioned experimental results with our model, we have assumed the validity of the Vegard's law and calculated the average chemical composition of the heterostructures from the x-ray-diffraction data obtained before the etching process. Thus, the so-obtained average molar fraction x of InAs in one superlattice period for the first sample has been used for calculating the strains after the etching process. Unfortunately, for the second sample, x-ray-diffraction data before the etching process were not available. In this case we have chosen the average molar fraction x of AlAs which gives the best fit for the experimental average strain data after the etching process. The obtained results are reported in Table II, where the theoretical strain values for the film before the etching process have been calculated by using the predictions of the deformation model for epitaxial layers as reported in Ref. 7. Considering that, due to the particular experimental conditions, the accuracy of the strain measurements, is of the order of 3×10^{-5} for perpendicular strains and of 1×10^{-4} for parallel strains, within these errors, our orthorhombic lattice deformation model is in very good agreement with the experimental results. Moreover, by using Vegard's law we obtain the same chemical composition for the sample before and after the etching process, using the tetragonal and the orthorhombic deformation models, respectively.

These results demonstrate that, in both one-dimensional heterostructures, the lattice deformation is determined by the only boundary condition of coherence along the wire direction. In this way, the stress can be partially relaxed and, consequently, the strain energy density is reduced with respect to the pseudomorphic case. However, it is reasonable to suppose that the above-mentioned boundary condition is no longer valid near the wire/substrate interface. In fact, near the interface, the strain field tends towards the tetragonal strain values and, as shown schematicaly in Fig. 2, the deformation field is a combination of the orthorhombic (relaxed) and the tetragonal (bulk) strain fields. This conclusion is confirmed by the observation that the experimental average perpendicular deformation values are slightly greater than the theoretical values, contrary to the parallel deformation values which are slightly smaller.

Treacy and Gibson[11] have shown that in thinned superlattices the lattice tends to relax where the relaxation degree increases with increasing distance from the interface. Moreover, the distance from the interface, at which the lattice parameter can be considered fully relaxed, depends on the lateral dimension of the heterostructure. However, comparing the theoretical predictions of our model, which does not consider the particular lattice deformation at the quantum-wire–substrate interface, with the experimental x-ray-diffraction data, we conclude that the tetragonal contribution to the total average strain seems to be negligible in our samples (see Table II). The ratio width/height for the examined samples is always less than 0.6. But, for greater values of this ratio and/or of the lattice mismatch, the tetragonal contribution near the interface may become not negligible. The development of a model which describes the elastic lattice relaxation at the quantum-wire–substrate interface as a function of the distance from the interface and the width of the wires is in progress and will be reported elsewhere.[12]

TABLE II. Experimental and theoretical results for the orthorhombic deformation in quantum-wire heterostructures. QW indicates the quantum wires, while EL refers to the epitaxial layer before the etching process. x is the molar fraction of indium for Ref. 5 and of aluminum for Ref. 6.

	$(10^{-3}\Delta d/d)_{\perp}$ of the QW	$(10^{-3}\Delta d/d)_{\parallel}$ of the QW	$(10^{-3}\Delta d/d)_{\perp}$ of the EL	$(10^{-3}\Delta d/d)_{\parallel}$ of the EL
Experimental results (Ref. 5)	2.20±0.03	1.4±0.1	2.86±0.03	0
Theoretical results for Ref. 5	2.17 ($x=0.0225$)	1.5 ($x=0.0225$)	2.86 ($x=0.0225$)	0
Experimental results (Ref. 6)	0.59±0.03	0.4±0.1	/	0
Theoretical results for Ref. 6	0.57 ($x=0.275$)	0.4 ($x=0.275$)	/	0

V. CONCLUSIONS

In this work we studied theoretically the lattice deformation of quantum-wire heterostructures with cubic symmetry on arbitrarily-oriented substrates. The elastic strain and the stress-tensor components are calculated by assuming that the layers with different lattice constants are coherent only along the wire direction, and applying Hooke's law. We show that, also for high-symmetry substrate orientations when the wire direction is a low-symmetry one, it is possible to obtain one shear strain element different from zero, leading to a monoclinic lattice deformation. Conversely, for the high-symmetry wire directions [001] and [110], the lattice deformation is either tetragonal or orthorhombic, depending on the fact that the axes $\mathbf{x}_1$ and $\mathbf{x}_3$ may or may not be equivalent crystallographic directions. In each case, the stress can be partially relaxed and, consequently, the strain energy density is reduced with respect to the pseudomorphic condition. Moreover, for [111]-oriented or arbitrarily [*jkm*]-oriented substrates the deformation can be also of lower symmetry than monoclinic. The theoretical results obtained for the case of an orthorhombic lattice deformation ([001]-oriented substrate and [011]-oriented quantum wires), are found to be in very good agreement with the experimental evidences reported previously.

[1]C. P. Kuo, S. K. Vong, R. M. Cohen, and G. B. Stringfellow, J. Appl. Phys. **57**, 5428 (1985).
[2]J. M. Hinckley and J. Smith, Phys. Rev. B **42**, 3546 (1990); Appl. Phys. Lett. **60**, 2694 (1991).
[3]C. Mailhiot and D. L. Smith, Phys. Rev. B **35**, 1242 (1987); Rev. Mod. Phys. **62**, 173 (1990), and references therein.
[4]E. A. Fitzgerald, Mater. Sci. Rep. **7**, 87 (1991), and references therein.
[5]L. Tapfer, G. C. La Rocca, H. Lage, O. Brandt, D. Heitmann, and K. Ploog, Appl. Surf. Sci. **60/61**, 517 (1992).
[6]L. Tapfer, G. C. La Rocca, H. Lage, R. Cingolani, P. Grambow, A. Fischer, D. Heitmann, and K. Ploog, Surf. Sci. **267**, 227 (1992).
[7]L. De Caro and L. Tapfer, Phys. Rev. B **48**, 2298 (1993).
[8]J. F. Nye, *Physical Properties of Crystals* (Oxford University Press, Oxford, 1964), pp. 93–109 and 131–149.
[9]E. Anastassakis and E. Liarokapis, Phys. Status Solidi B **149**, K1 (1988).
[10]The used GaAs stiffness constants have been taken from Landolt-Börnstein, Numerical Data and Functional Relationships in Science and Technology, New Series Group III, Vol. 17, Pt. a, edited by O. Madelung, M. Schulz, and H. Weiss (Springer-Verlag, Heidelberg, 1982).
[11]M. M. J. Treacy and M. Gibson, J. Vac. Sci. Technol. B **4**, 1458 (1986).
[12]L. De Caro and L. Tapfer (unpublished).